energies

MDPI

Article

Investigating Pressure Patterns in Transformer Tanks after an Interturn Short Circuit: A Finite Element Approach

Mingming Han [1], Mengzhao Zhu [1], Zhaoliang Gu [1], Qizhao Zhang [2], Ruxue Zhao [2] and Hongshun Liu [2,*]

[1] Electric Power Science Research Institute, State Grid Shandong Electric Power Company, Jinan 250002, China; 202334758@mail.sdu.edu.cn (M.H.); 202334792@mail.sdu.edu.cn (M.Z.); 202114592@mail.sdu.edu.cn (Z.G.)

[2] School of Electrical Engineering, Shandong University, Jinan 250061, China; zqz@mail.sdu.edu.cn (Q.Z.); 202334806@mail.sdu.edu.cn (R.Z.)

* Correspondence: lhs@sdu.edu.cn

Abstract: When an inter-turn short-circuit fault occurs during the operation of a transformer, the arc generates energy that causes the temperature in the tank to rise. This in turn increases the temperature of the insulating oil, vaporizing it, and the rising pressure in the tank acts on the tank such that it can easily explode. The arc energy is related to the initial pressure of the gas and its production in the tank. The pressure wave propagates in insulating oil, and the transient pressure at any point in the path of the pressure wave is the superposition of vectors of forward- and backward-traveling waves. The authors of this study applied a finite element simulation software to establish a model of the transformer tank and used it to analyze the changes in pressure in the tank and on the wall as well as the factors influencing this phenomenon. The results show that the wall pressure of the transformer increases with time after the failure of the interturn short circuit. The pressure wave travels from the initial position of the arc to the periphery and decreases with diffusion effects. The influence of pressure on the transformer tank can be reduced by selecting an appropriate location for the pressure-release valve and can in turn prevent the tank from rupturing due to the impact of rising pressure.

Keywords: transformer; arc discharge; fuel tank; stress field; finite element simulation

check for updates

Citation: Han, M.; Zhu, M.; Gu, Z.; Zhang, Q.; Zhao, R.; Liu, H. Investigating Pressure Patterns in Transformer Tanks after an Interturn Short Circuit: A Finite Element Approach. *Energies* **2024**, *17*, 564. https://doi.org/10.3390/en17030564

Academic Editor: Adrian Ilinca

Received: 27 September 2023
Revised: 15 January 2024
Accepted: 16 January 2024
Published: 24 January 2024

1. Introduction

Transformers are among the most important components of transmission and distribution systems, and they are the key equipment used for power transmission. When an inter-turn short-circuit fault occurs inside a transformer, the arc releases energy, causing the temperature of the surrounding insulating oil to rise instantaneously such that it vaporizes, rapidly increasing the pressure inside the tank [1]. Once the pressure exceeds the limit that can be borne by the tank structure, it cracks, and the combustible gas inside the tank comes into contact with oxygen. This can lead to ignition and an explosion that can damage the equipment, cause a fire at the substation, and lead to regional power failure. Serious accidents of this kind can cause casualties, significant economic loss, and power failure [2]. Currently used electrical relay protection for large power transformers mainly includes current-break protection and zero-sequence current protection. However, although the internal fault current in case of inter-turn short-circuit faults is large, the reflected line current is not [3]. Therefore, there is a "blind spot" in the protection provided for the transformer in case of inter-turn and inter-layer short-circuit faults. The development of non-electrical relay protection technology plays a critical role in fault protection in cases of inter-turn and inter-layer short-circuiting [4]. The strong, local electric field formed by the short-circuiting of the winding and the layers of the transformer as well as the deterioration of the insulation oil often induce the breakdown of the insulation. This can lead to high-energy arc failure, and the arc discharge causes the insulation structure to generate a violent physical and chemical reaction. The high gas yield obtained by the high arc temperature causes the dissolved gas to escape in the form of bubbles and rapidly expand and accumulate in the transformer. The pressure-release valve cannot be used in this case to release the high pressure inside the transformer, which is at risk of an explosion that can cause a fire [5–8]. The expansion of bubbles caused by arc discharge and the rise in pressure caused by the accumulation of gas are the direct causes of the explosion of the transformer tank. A strong electric field arises before arc discharge, and the temperature and pressure inside the transformer continue to increase during arc development until an explosion occurs. The process of evolution of arc discharge in the transformer before it explodes involves the coupling of a strong electromagnetic field, a high-temperature field, and a strong stress field.

A considerable amount of research has been devoted to solving the above-mentioned problems. In the context of the mechanism of evolution of discharge in transformer oil, the IEEE's Transformer Explosion and Prevention Group found that the arc voltage can be estimated based on the length of the discharge arc. The risk of explosion of the fuel tank of the transformer can then be evaluated based on the arc energy [9]. However, the arc is only the initial stage as a source of energy generation, and there are still multiple processes to go through in the final evaluation of the risk of fuel tank explosion. Additionally, the accuracy of this assessment method is relatively poor. Researchers have also used optical images of the development of flow under AC voltages of different amplitudes to investigate the mechanisms of spatiotemporal evolution of the flow [10]. The common morphology of stream discharge has been described, and such characteristic parameters as the stopping length of discharge and its cross-sectional have been compared and analyzed by studying the dynamic characteristics of the pre-breakdown discharge of the insulation oil under an impulse voltage [11]. In the context of the production of arc gas in the insulation oil and the stress acting on the tank, researchers have investigated the mixed combustible gas generated by the action of arc discharge on the insulation oil under different conditions. They have characterized the risk of detonation owing to the mixed gas by calculating the limit of explosion [12]. The above references focus on the study of the morphological characteristics and physical mechanisms of flow discharge, partial discharge, and arc development in oil, as well as the analysis of the characteristics of arc gas production. There is a lack of research on the law of pressure development, and no analysis of tank bursting.

A simple empirical equation has been formulated to express the rise in pressure in the transformer tank due to the arc failure of the transformer [13]. Moreover, the dependence of the volume of bubbles, which influences the rise in pressure, on the arc energy has been examined to determine the volume of bubbles generated per unit energy [14]. The references focus on the analysis of the composition of the gas generated after the combustion of transformer oil, as well as the study of stress on the tank, lacking an analysis of the process from pressure wave generation to transmission.

The performance of transformer tanks of varying shapes has also been assessed under the action of fault-induced pressure in the case of arc discharge [15], but without considering the compressibility and viscosity of the insulation oil. This was combined with test data and an empirical formula to calculate the conditions of an increase in the voltage of transformer tanks of different sizes under different arc faults [16,17]. Additionally, the intensity of the measured pressure waves is the most critical characteristic [18–22]. Although the above references have analyzed and calculated the energy of arc faults and the final force, they lack the connection between macroscopic fault characteristics such as inter-turn short circuits and inter-layer short circuits in the internal winding of transformers and microscopic arc discharge laws, and they also lack an analysis of the propagation mechanism of pressure waves inside.

The above shows that research in this area has explored the characteristics of abnormal discharge in transformer oil, including its form, the generation of degraded gas, and its spatiotemporal evolution. Researchers have derived the internal changes in pressure caused by arc discharge-induced fault in the fuel tank, and they have used it to examine the temperature, vibrations, and deformation of the tank and related characteristics.

In summary, prevalent research in this area has placed a greater emphasis on the physical mechanisms of the streamer and the partial discharge of the transformer oil. Although arc discharge is the main cause of transformer tank explosions, the currently available results do not organically link the action of the arc with the development of pressure in the tank. The law of pressure transfer in the transformer tank due to the presence of a large number of bubbles following arc discharge thus remains unclear.

This paper takes the temperature and stress fields of the arc discharge caused by short-circuiting of the turns of the winding in the transformer oil as the object of research. We theoretically analyze and deduce the characteristics of gas production caused by the short-circuiting of the turns based on the topology of the circuit, the AC system, and the properties of the insulation oil to establish a quantitative relationship between the short-circuiting of turns of the winding and the law of arc discharge at the macroscopic level. Moreover, we analyze and optimize the generation and action of the source of pressure on the wall of the tank and its internal components at the systemic level. We establish a model of the transfer of pressure in the transformer and use a finite element software to simulate the pressure and temperature fields in the tank under the action of the electric arc to verify the theoretical results. We seek to explain the law of generation of pressure by the gas in the tank as well as its transmission under an arc fault and propose an explosion-proof transformer tank to ensure the operational safety of the HVDC (high-voltage direct current) transmission system.

This paper is structured as follows: Section 2 mainly discusses the arc discharge characteristics and gas generation mechanism in transformer insulation oil. In Section 2.1, the calculation process of arc energy generated under a transformer inter-turn short circuit fault is derived, taking into account the arc energy and its influencing factors. Due to the influence of gas production on the initial pressure value, the relationship between the arc energy and gas production characteristics is analyzed in Section 2.2, and the process of temperature and pressure transmission in oil inside the box under the action of arc is analyzed in Section 2.3. Section 3 mainly provides a detailed introduction to the process of establishing a finite element model using simulation models, while Section 4 is divided into three sections to analyze the simulation results. Section 4.1 presents the results and analysis of the pressure wave and the pressure on the tank, and Section 4.2 analyzes the final effect of changing the position of the arc on the pressure value on the tank. Section 4.3 introduces the relationship between the opening position of the pressure relief valve and the pressure bearing.

2. Characteristics of Arc Discharge and Gas Production in Transformer Oil

2.1. Arc Energy in the Case of Short-Circuiting between Turns of Winding

A small number of turns can usually lead to the breakdown of insulation oil and arc discharge in the case of a short-circuit fault in the transformer oil. When a fault occurs, insulation damage occurs in the part of the winding of the transformer where the turn-to-turn short circuit occurs. The damaged position of the winding and insulating oil are broken down under the action of a large electric field (voltage), and gas discharge in the insulating oil occurs. A short circuit between turns in the transformer generates an arc discharge in the oil. At this time, this part of the faulty winding is short-connected, and arc generation renders it a closed loop. This is equivalent to generating a new short-circuit transformer with a high ratio of turns of the coil, as shown in Figure 1. N_1 in the figure represents the number of turns on the primary side of the transformer, N_2 is the number of turns on its secondary side, and N_b is the number of turns between the occurrence of the inter-turn short-circuiting. Therefore, the winding of the original transformer becomes a winding composed of an inter-turn short-circuit winding and the remaining part in parallel.

We now analyze the equivalent arc resistance r_arc with respect to the flowing current i_arc from the point of view of the short-circuited turns. Given the saturation factor of the transformer, the magnetic flux in the core does not change significantly, even if a turn-to-turn short-circuit occurs. It is assumed in Figure 1 that the potential induced on the primary side is u_1 and its impedance is Z_1. Then, the potential induced by the short-circuited turns N_b is $u_{Nb} = (N_b/N_1)\, u_1$, its impedance, $Z_b = Z_1(N_b/N_1)^2$, is very low, and this causes a large short-circuit current $i_{12} = u_{Nb}/Z_b$.

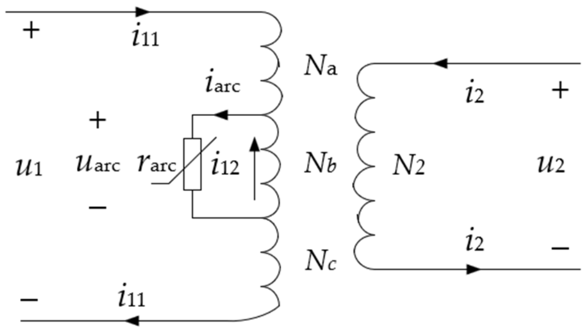

Figure 1. Equivalent circuit of a single-phase double-winding short-circuit fault in a transformer.

According to the empirical formula for its calculation, the arc energy E(J) is an integral function of the arc current $i_{arc}(t)$, arc voltage $u_{arc}(t)$, and time t_{arc}(s):

$$E = \int_0^{\mathrm{arc}} u_{\mathrm{arc}}(t) \cdot i_{\mathrm{arc}}(t) dt \tag{1}$$

It is necessary to know the functional relationship between the voltage and the current at both ends of the arc over time.

According to the analysis in Figure 1, the arc current $i_{arc}(t)$ can be calculated as:

$$i_{\mathrm{arc}}(t) = i_{11}(t) + i_{12}(t) \tag{2}$$

where i_{11} is the current passing through the winding when an arc fault occurs. Assuming that the rated current passing through the coil of the transformer is I_n, i_{11} can be given as follows:

$$i_{11}(t) = \sqrt{2} I_{\mathrm{n}} \sin(2\pi f t + \varphi) \tag{3}$$

When $i_{12} = u_{Nb}/Z_b$, we can rewrite i_{12} as follows when the rated voltage of the coil of the transformer is U_e:

$$i_{12}(t) = \frac{\sqrt{2}}{Z_1} \cdot \frac{N_1}{N_{\mathrm{b}}} U_{\mathrm{e}} \sin(2\pi f t + \varphi) \tag{4}$$

The magnitude of the current of the arc can then be expressed as:

$$i_{\mathrm{arc}}(t) = \left(\sqrt{2} I_{\mathrm{n}} + \frac{\sqrt{2}}{Z_1} \cdot \frac{N_1}{N_{\mathrm{b}}} \right) \cdot \sin(2\pi f t + \varphi) \tag{5}$$

The above magnitude of the arc current is derived by ignoring the changes in the impedance of the new short-circuit transformer generated by the short circuit. The impedance of the arc generated in the circuit is nonetheless dynamic. Once the arc resistance is considered, the magnitude of the arc current i_{12}' is as follows:

$$i_{12}'(t) = \frac{\sqrt{2} N_1 N_{\mathrm{b}}}{Z_1 {N_{\mathrm{b}}}^2 + r_{\mathrm{arc}} {N_1}^2} U_{\mathrm{e}} \sin(2\pi f t + \varphi) \tag{6}$$

At this time, the magnitude of the arc current is:

$$i_{\mathrm{arc}}'(t) = \left(\sqrt{2} I_{\mathrm{n}} + \frac{\sqrt{2} N_1 N_{\mathrm{b}}}{Z_1 {N_{\mathrm{b}}}^2 + r_{\mathrm{arc}}(t) {N_1}^2} U_{\mathrm{e}} \right) \cdot \sin(2\pi f t + \varphi) \tag{7}$$

The arc current generated by the inter-turn short circuit obtained above in (7) is related not only to the rated voltage current of the operating transformer but also to the number of turns of the short-circuit point and the dynamic resistance of the arc.

The energy produced by the arc can be obtained using (1) based on the current and voltage of the arc. The arc voltage is related to the arc length given in (8). Figure 2 shows that the voltage of a 100 mm long arc was approximately 1000 V, and the curve fitted at each point was roughly a line representing direct proportionality [23]:

$$U_{\text{arc}} = 10 \times L_{\text{arc}} \tag{8}$$

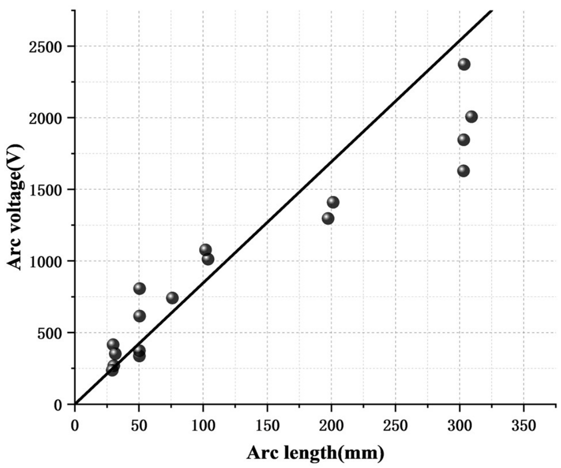

Figure 2. Diagram of the relationship between arc length and voltage.

The arc energy generated by the inter-turn short-circuiting can then be expressed as:

$$W_{\text{arc}} = 10L_{\text{arc}} \int_0^{t_{\text{arc}}} \left(\sqrt{2}I_{\text{n}} + \frac{\sqrt{2}N_1 N_{\text{b}}}{Z_1 {N_{\text{b}}}^2 + r_{\text{arc}}(t){N_1}^2} U_{\text{e}} \right) \cdot |\sin(2\pi f t + \varphi)| dt \tag{9}$$

According to (9), the number of turns of the short-circuit point N_{b}, arc time t_{arc}, arc length L_{arc}, the transformer used, rated current I_{n}, and rated voltage U_{e} are the main variables influencing the arc energy.

By taking the arc time t_{arc} as the independent variable, we plot the above parameters to explore the changing trend of arc energy with increasing arc time, as shown in Figure 3.

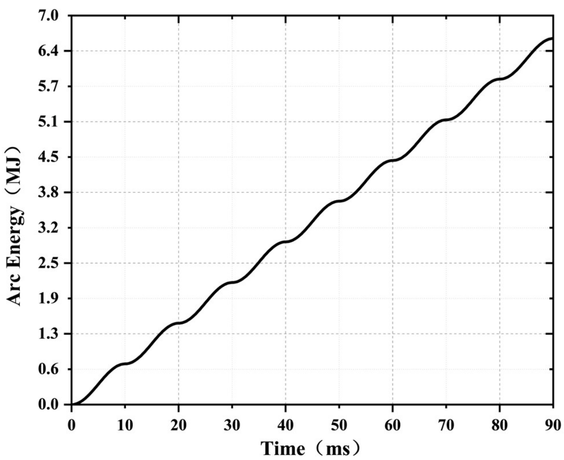

Figure 3. Trend of variations in the arc energy with arc ignition time.

The curve of the arc energy obtained in the case of 5% inter-turn short-circuiting in simulations of the single-phase high-voltage winding of the transformer shown in Figure 3 demonstrates that the energy released by the arc is gradually accumulated over time.

2.2. Law of the Development of Arc Energy under the Action of Multiple Factors

In reference [22], the approximate relationship between the internal arc fault energy of the transformer and the gas production is summarized by experiments performed using (10), where β is the coefficient of conversion, which is generally set to 0.44:

$$V_{\text{gas}} = \beta \ln(W_{\text{arc}} + \kappa) - \varphi \tag{10}$$

We assumed that a 5% inter-turn short-circuiting fault occurred in the single-phase high-voltage winding of the transformer. The total number of turns of the high-voltage winding was 531 (N_1 = 531), the number of turns of the short circuit was 27 (N_b = 27), the rated current of the high-voltage winding was 315 A (I_n = 315 A), and the rated voltage was 220 kV (U_e = 315 A). The high-voltage winding was 1750 mm high, which means that each turn of the winding was 3.3 mm high. The winding of the turns of the short circuit was 89 mm high, its impedance was 90.79 Ω, and the resistance of the arc was on the order of mΩ.

We used the type of fault and turns of the short circuit N_b as independent variables to obtain (11):

$$W_{\text{arc}} = 10L_{\text{arc}}\left(\sqrt{2}I_n + \frac{\sqrt{2}N_1}{Z_1 N_b}U_e\right)\int_0^{t_{\text{arc}}} |\sin(2\pi f t + \varphi)|dt \tag{11}$$

Because the arc length L_{arc} is directly proportional to the number of turns of the short circuit, L_{arc} can be expressed as kN_b. Formula (11) can thus be approximated as (12):

$$W_{\text{arc}} = \left(10\sqrt{2}kN_b I_n + \frac{10\sqrt{2}kN_1}{Z_1}U_e\right)\int_0^{t_{\text{arc}}} |\sin(2\pi f t + \varphi)|dt \tag{12}$$

It is evident from (12) that the relationship between the number of turns of the short circuit N_b and the arc energy was a linear function. That is, the cumulative fault-induced arc energy increased approximately linearly with the number of short-circuit turns over time. Figure 4 shows a plot generated using different numbers of turns of the short circuit in the formula. It is clear that the slope of the two curves was closely related to the severity of the fault; that is, the number of short-circuit turns.

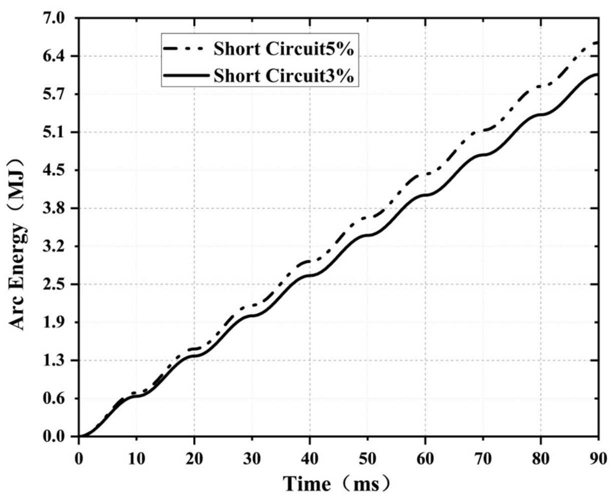

Figure 4. Changes in the arc energy over time with different numbers of short-circuit turns.

For gas production, (10) indicates that there is a logarithmic relationship between the gas production and arc energy. By substituting the arc energy Formula (12) into (10), the relationship between gas production and arc energy can be obtained, as shown in Figure 5.

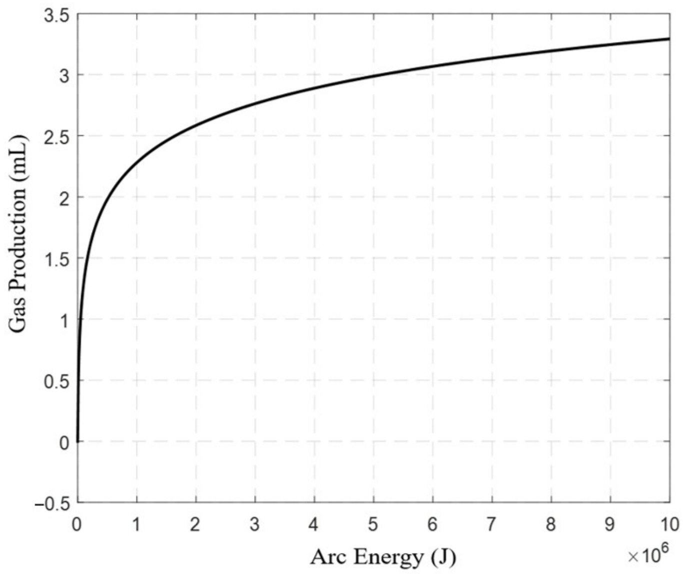

Figure 5. Relationship between arc energy and gas production.

A logarithmic relationship was observed between the fault-induced arc energy and gas production. When the arc energy reached a certain value, the slope of the curve decreased rapidly and gradually tended toward saturation. This was caused by the saturation of the arc during the vaporization of the insulating oil.

2.3. Pressure Transfer under the Action of Arc Energy

The temperature of the arc is related to the medium environment, and the dissociation and de-dissociation speed of the arc combustion are different in different media. The temperature near the arc was approximately 4000~5000 K [23–25], while the highest temperature at the center of the arc column was 10^4 K. The burning point of mineral oil that is generally used in the transformer is approximately 400 K. The insulating oil near the arc was instantly gasified and decomposed owing to the very high temperature. At this time, the energy released by the arc W_{arc} was mainly converted into energy absorbed by the decomposition of the insulation oil. W_{arc} radiated into the surrounding heat, and the energy absorbed by the evaporation of the oil led to the production of gas.

$$W_{\text{arc}} = W_{\text{oil}} + W_{\text{gas}} + W_{\text{rad}} \tag{13}$$

According [26–32], the energy distribution mainly comes from W_{gas}.

Under standard pressure, when the arc energy is 1 kJ, the corresponding gas production is approximately 5.8×10^{-4} m^3/kJ. According to the above analysis, the transformer data in Section 2.2 is input into Formulas (10) and (12) to calculate the amount of gas volume produced, which is approximately 10^{-6} m^3 by 1 kJ of arc energy. This is much smaller than the gas produced under standard pressure and could thus be ignored when calculating the fluctuations in the temperature of oil. According to the law of heat conduction, the transfer of heat to and the rise in the temperature of the insulating oil according to the distance from the arc can be calculated using the following formula:

$$T_{\text{oil}}{}' = \frac{\mu S}{m c_{\text{oil}} L}\left(T_{\text{arc}} - T_{\text{oil}}\right) + T_{\text{oil}} \tag{14}$$

T_{arc} represents the temperature of the arc and the thermal conductivity, which is generally 0.15 W $(\mathrm{m}\cdot\mathrm{K})^{-1}$ in insulating oil [33]. S represents the area of heat transfer between the insulating oil and the arc, T_{oil} represents the initial temperature of the insulating oil, $T_{\mathrm{oil}}{}'$ represents its real-time temperature, and L represents the distance between the insulating oil and the arc during heat conduction. m is the unit mass of the insulating oil and c_{oil} is its specific heat capacity. It is clear from (14) that heat transfer in the insulation oil was mainly influenced by the arc heat, and it gradually decreased with an increase in its distance to the arc.

The volume expansion of insulating oil has a hysteresis effect relative to the production of gas. The transient pressure of gas produced by the arc continues to drastically increase with the discharge time of the high-energy arc. Therefore, a high pressure was obtained at the interface of the gas and the insulating oil during the phase transition reaction, which spread around in the form of a pressure wave in the oil and acted on the wall of the tank. This caused the tank to bear the corresponding stress and deform once the pressure exceeded a certain limit, or to even accumulate too much elastic energy in a short time such that it burst. The change in the phase of the insulating oil from liquid to gas followed the law of the conservation of mass. The mass of the vaporized oil could then be obtained according to the mechanism of vaporization-induced evaporation of oil:

$$m_{\mathrm{og}} = \frac{W_{\mathrm{gas}}}{c_{\mathrm{oil}}\left(T_{\mathrm{gas}} - T_{\mathrm{oil}}\right) + \frac{\Delta Q^{*}}{m}} \tag{15}$$

where m_{og} is the mass of the insulating oil undergoing a phase change, T_{gas} represents the transient temperature of the generated gas, and ΔQ^{*} is the latent heat of vaporization of the insulating oil per unit mass (the heat absorbed by a certain liquid per unit mass during vaporization when the temperature is constant). We analyzed the components of the gases produced by the combustion of the arc in the insulation oil. They consisted of 7.85% ethylene, 13.96% methane, 14.87% methanol, 22.17% acetylene, and 30.77% propane [34]. The molar mass of the gas generated in the insulation oil was approximately 28.99 g/mol. According to the ideal gas equation, its pressure can be calculated as follows:

$$p_{\mathrm{gas}} V_{\mathrm{gas}} = nRT_{\mathrm{gas}} \tag{16}$$

In (15), n represents the amount of matter and R represents the molar gas constant, with a typical value of 8.31451 J/(mol·K).

The transient pressure of the generated gas can then be obtained by substituting (10) and (15) into (16):

$$p_{\mathrm{gas}} = \frac{W_{\mathrm{gas}} R T_{\mathrm{gas}}}{28.99 \times V_{\mathrm{gas}}\left[c_{\mathrm{oil}}\left(T_{\mathrm{gas}} - T_{\mathrm{oil}}\right) + \Delta Q^{*}\right]} \tag{17}$$

Figure 5 shows that when the energy released by arc combustion over time accumulated to reach a certain value, the gas production approached saturation. We thus assumed that the volume of gas produced did not change when calculating the transient pressure and the transfer of internal pressure. The initial pressure of the generated gas was approximately proportional to the arc energy. The initial difference in pressure at the position of the arc in the insulation oil was as follows:

$$\Delta p = p_{\mathrm{gas}} - p_0 - \rho_{\mathrm{oil}} g h \tag{18}$$

where p_0 is the atmospheric pressure, 1.01325×10^5 Pa; ρ_{oil} is the density of the insulating oil; g is the acceleration due to gravity; and h is the depth with respect to the surface of the oil at which the arc discharge occurred. The derivation of some of the above equations is listed in the Appendix A.

We analyzed the propagation of the pressure wave in the insulating oil. We regarded the generated gas pressure as a source of transient pressure that could provide initial shock-induced excitation in the oil tank $P_{\mathrm{v}}(t)$. The coupling of two-phase gas–liquid flow was calculated by using the volume function model (VOF). The shock induced by the source of transient pressure $P_v(t)$ in the tank was transmitted to the insulating oil in the form of waves and acted on the wall of the tank, causing it to strain.

The insulating oil was compressible and viscous. The greater the viscosity of the fluid, the worse its fluidity; therefore, the viscosity of the oil weakened the transmission of the pressure wave. Figure 6 shows that the compressibility of the oil caused the pressure wave to propagate with a velocity v. When a difference in pressure was obtained between the gas and the surrounding insulating oil, the pressure at a distance of δx from the gas increased instantaneously, Δp. The insulating oil at this distance was then transferred to its adjacent liquid surface δx, causing its pressure to increase by Δp and its velocity to change from zero to v. This process occurred in each layer to form an initial pressure wave with a magnitude Δp that propagated at a velocity v toward the surrounding walls of the tank.

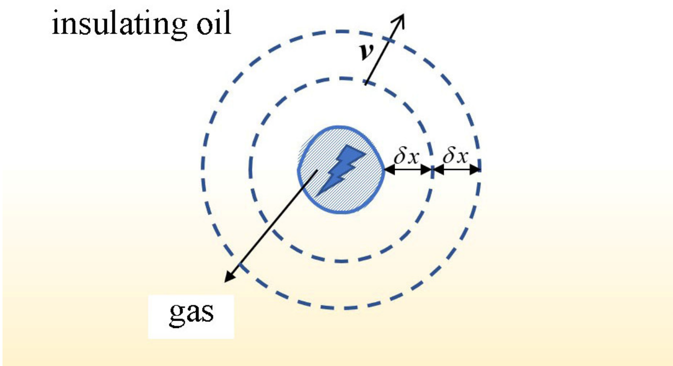

Figure 6. Initial propagation of the pressure wave.

Figure 7 shows that the propagation of the pressure wave increased the pressure of the insulation oil by Δp. The pressure wave traveled over a distance of $\sum\delta x = v\Delta t$, causing the pressure of water to rise within this distance by Δp, while $p_0 + p_{\text{oil}}gh$ remained unchanged in the section in which the wave did not propagate. There is no reflection if a source of transient pressure $P_v(\text{t})$ is generated in a frictionless and infinitely large container, and the pressure wave is indefinitely transmitted. However, the energy of the pressure wave continuously decreased during propagation in the actual transformer tank due to the influence of the viscous insulation oil and the elastic walls of the tank. Energy was thus transmitted to the walls of the tank.

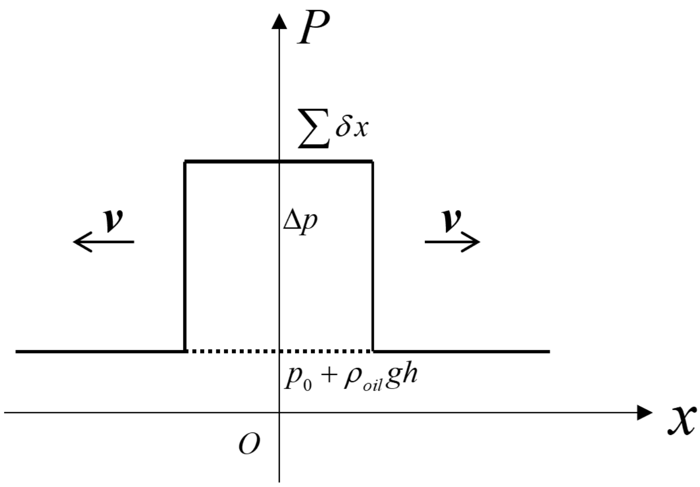

Figure 7. Initial distance of propagation of the pressure wave and the changes in pressure.

3. Finite Element Simulation of Pressure in a Tank

We used a finite element simulation software to represent the changes in the pressure in the transformer tank once an internal fault had occurred. We simulated a transformer tank by considering only three key components of the transformer. The overall geometric model of the tank is shown in Figure 8. The length of the tank was 4 m, its width was 1.4 m, and its height was 2 m. A model of the core and the winding was provided inside the tank, and stiffeners were installed at suitable positions outside it.

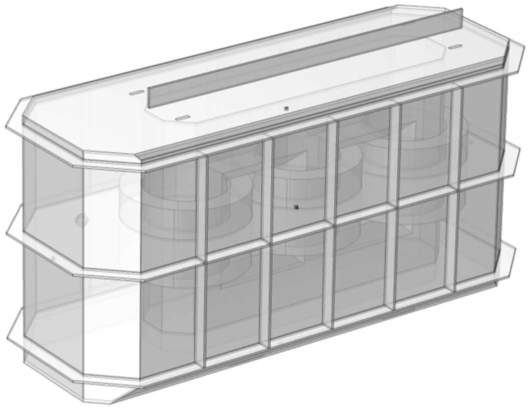

Figure 8. Geometric model of the transformer tank.

The model of the tank can be divided into two parts: the tank itself and the winding with an iron core. The relevant models are shown in Figures 9 and 10.

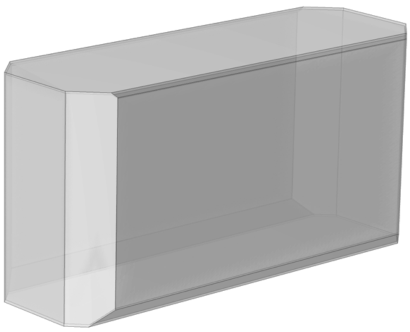

Figure 9. Geometric model of the housing (tank) of the transformer tank.

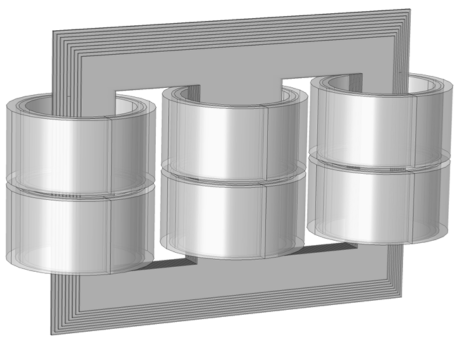

Figure 10. Geometric model of the winding of the transformer tank with an iron core.

The thickness of the wall of the tank was set to 16 mm. The model was used to simulate the propagation of the pressure wave under the wall.

The model of the iron core shown in Figure 10 was composed of multiple sheets of silicon and steel that were superimposed on each other, and the winding circuit was simulated by using the virtual circuit in the simulation software. The coil can be divided into primary and secondary coils. This model was used to simulate the distribution of force under the propagation of the pressure wave.

We varied the position of occurrence of the initial arc (that is, the initial position of generation of bubble-induced pressure) in the finite element simulations, and we set multiple probes at different positions in the tank and its wall for measurements, as shown in Figures 11 and 12.

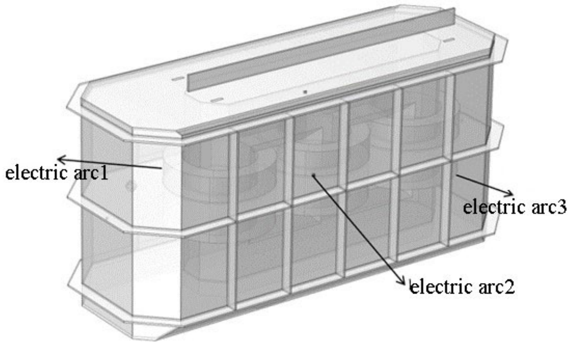

Figure 11. Positions of occurrence of the initial arc in the transformer tank.

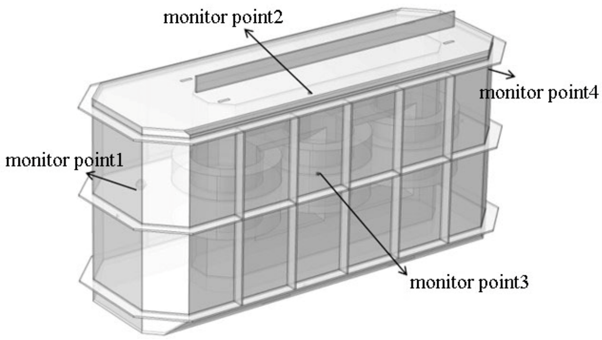

Figure 12. Monitoring points of the transformer tank.

A finite-element mesh division was used, as shown in Figure 13. We simulated the transfer of pressure inside the transformer tank under the action of the source of transient pressure and the distribution of pressure on the wall of the tank according to the initial position of the arc, and we analyzed the propagation of the pressure wave based on a diagram of the contours of the pressure distribution.

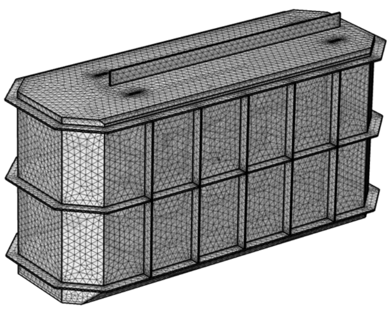

Figure 13. Finite-element mesh model of the transformer tank.

4. Law of Change in Pressure Field of a Tank and the Factors Influencing It

4.1. Simulation of Propagation of a Pressure Wave and Pressure on the Tank

The three-dimensional geometric model and finite element mesh generation model of the transformer are shown in Figures 12 and 13, mainly composed of the internal iron core and winding and the external tank. The simulation model is constructed according to a certain proportion based on the actual transformer size, and the geometric dimensions of the model are shown in Table 1 below.

According to the CFL principle [35], the finite element calculation time step must be shorter than the propagation time of pressure waves in two adjacent grid elements. In this paper, the model is divided into a total of 403,405 tetrahedral elements, and the simulation step size is selected as 2 μs. The calculation time for a single simulation of the example is several hours.

Table 1. Geometric structure and parameters of the transformers.

Parameter	Numerical Value
Tank length/mm	4000
Tank height/mm	2000
Tank width/mm	1400
Tank wall thickness/mm	16
Elastic strain limit	0.1775%
Yield stress/MPa	355
Elastic modulus/GPa	200
Poisson's ratio	0.3

In addition, using the COMSOL6.0 acoustic structure coupling model, the acoustic property parameters of each material in the model are set as shown in Table 2.

Table 2. Acoustic property parameters of transformer model.

Position	Material	Density/(kg/m^3)	Sound Velocity/(m/s)
Winding	Copper	8900	3810
Iron core	Iron	7600	5100
Transformer insulation oil	Mineral oil	850	1260

Inter-turn short-circuit faults occur commonly in the winding of the power transformer, which can cause significant damage. We chose position 2, as shown in Figure 12, as the site of the occurrence of the initial arc to analyze the propagation of the pressure wave as well as the pressure on the tank. The simulated distribution of the isosurface of the pressure in the tank and the pressure on its wall are shown in Figures 14 and 15, respectively. Position 2 was located in the middle of the tank, making our analysis adequately representative.

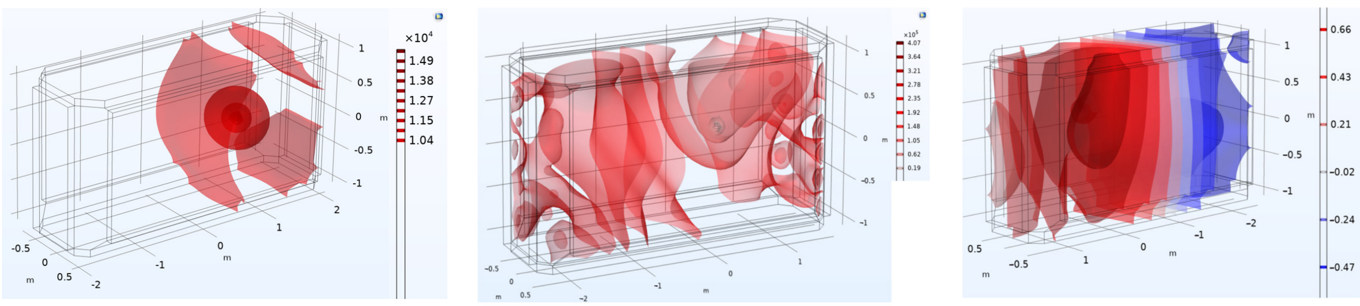

(**a**) t = 1 ms (**b**) t = 6 ms (**c**) t = 10 ms

Figure 14. Distribution of the contours of pressure in the transformer tank.

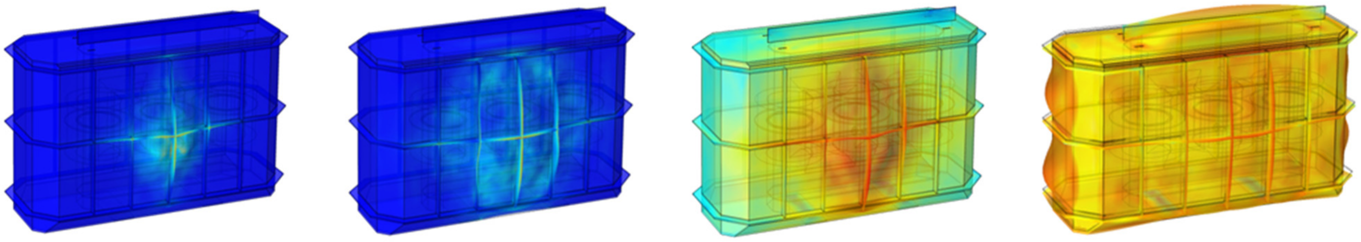

(**a**) t = 1 ms (**b**) t = 5 ms (**c**) t = 20 ms (**d**) t = 60 ms

Figure 15. Results of simulations of the changes in pressure on the wall of the transformer tank over time.

The red color in the diagram of the isosurface of pressure represents the forward-traveling wave, while blue represents the backward-traveling wave. Figure 14 shows that when the inter-turn short circuit of the winding occurred and the initial arc was formed at position 2, the pressure in the transformer tank first rose at position 2 because the insulating oil near it was instantly vaporized owing to the high temperature. Owing to the hysterical effect of the volumetric expansion of the insulating oil relative to the production of gas, the transient pressure of the gas increased drastically with the duration of discharge of the high-energy arc. The pressure in the tank thus increased over time from position 2 and spread around to gradually act on its wall.

Figure 15 shows that the pressure on the wall of the transformer tank continued to increase over time, spreading from the position of occurrence of the initial arc 2.1 ms after the fault had occurred. The side wall of the tank closest to the arc was deformed and expanded. Approximately 20 ms after the fault had occurred, the deformation had distributed throughout the body of the tank. The entire wall of the tank expanded and deformed under the action of pressure 60 ms after the initial fault had occurred.

It is clear from the distribution of the isosurface of pressure in the transformer tank and the diagram of variations in pressure on its wall over time that the pressure wave was transmitted from the initial position of the arc to the periphery after the fault had occurred. The pressure on the wall of the tank increased with time.

4.2. Relationship between the Initial Position of the Arc and the Pressure Distribution on the Wall of the Tank

The insulating oil in the transformer tank was viscous and compressible, thus weakening the transmission of the pressure waves. A comparison of the pressures at each monitoring point under three positions of the initial arc is shown in Figures 16–21. Arc 1 was located in the primary coil of the side winding, arc 2 was located in the primary coil of the middle winding, and arc 3 was located in the secondary coil of the side winding.

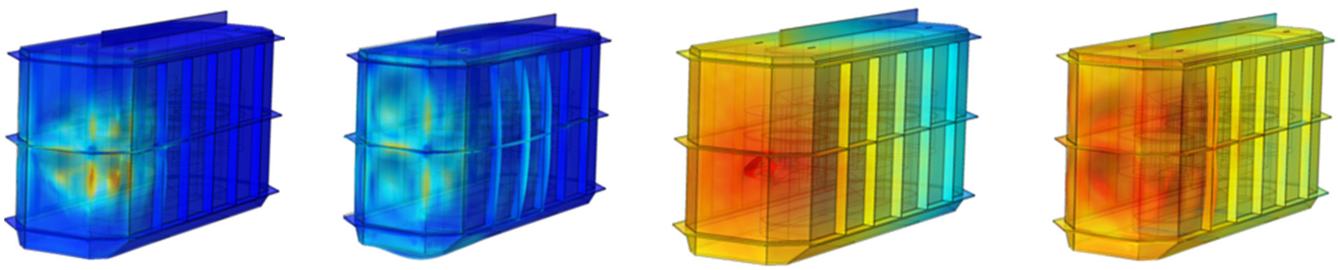

(**a**) t = 1 ms (**b**) t = 5 ms (**c**) t = 20 ms (**d**) t = 60 ms

Figure 16. Pressure on the wall of the tank over time in the case of arc 1.

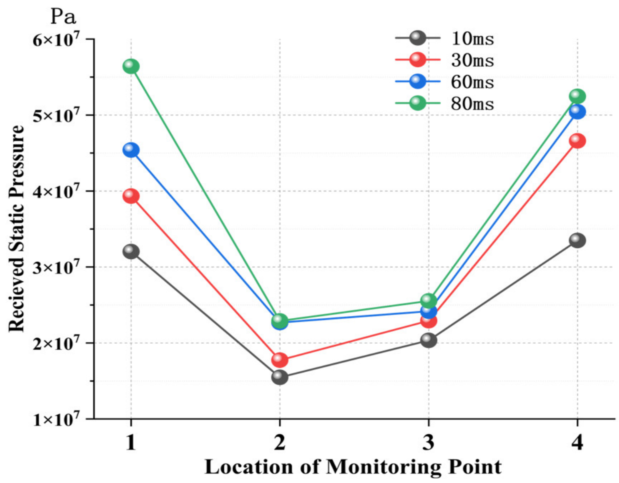

Figure 17. Magnitudes of pressure on the wall of the tank at multiple sites in the case of arc 1.

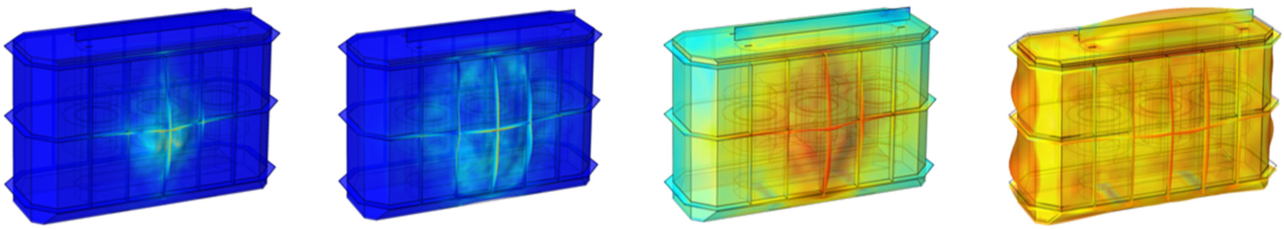

(**a**) t = 1 ms (**b**) t = 5 ms (**c**) t = 20 ms (**d**) t = 60 ms

Figure 18. Pressure on the wall of the tank over time in the case of arc 2.

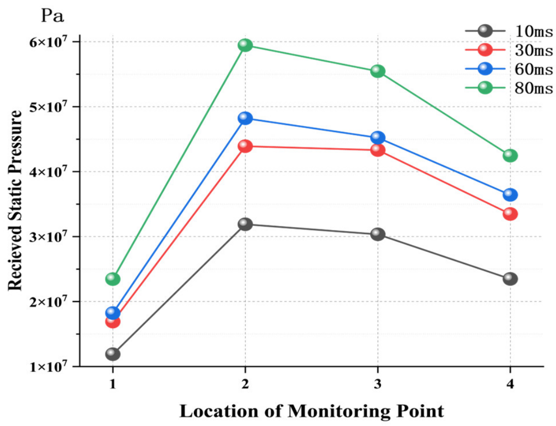

Figure 19. Magnitudes of pressure on the wall of the tank at multiple sites in the case of arc 2.

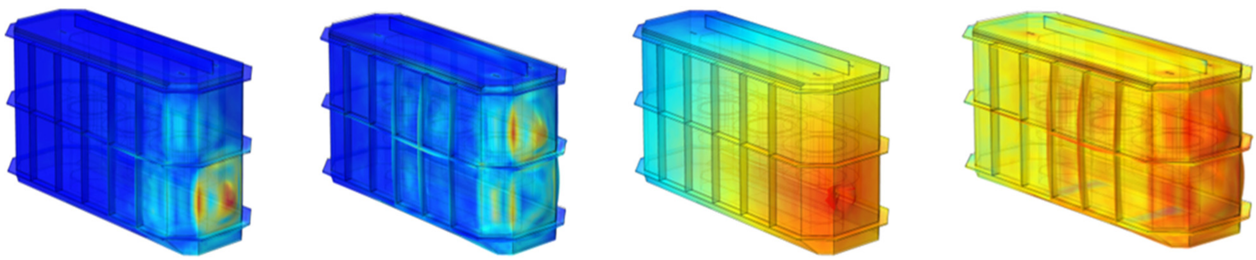

(**a**) t = 1 ms (**b**) t = 5 ms (**c**) t = 20 ms (**d**) t = 60 ms

Figure 20. Pressure on the wall of the tank over time in the case of arc 3.

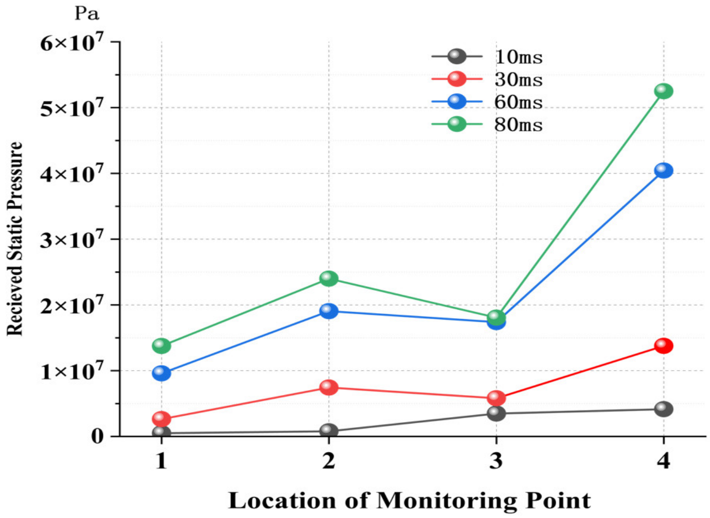

Figure 21. Magnitudes of pressure on the wall of the tank at multiple sites in the case of arc 3.

A comparison of the above three cases shows that the pressure measured at the monitoring point closest to the that of the occurrence of the arc was the highest, while that measured at the monitoring point farthest from it was the lowest. This is consistent with the previous derivation in Section 2.3. The viscosity of the insulating oil as well as the refraction and reflection of the internal components of the tank reduced the energy of the pressure wave in the oil.

4.3. Impact of the Position of the Pressure-Release Valve

The pressure-release valve is a device used to protect the transformer from excessively high pressure. The pressure in the tank rises sharply when the transformer oil in it vaporizes. If the pressure-release valve is opened in time, it can isolate part of the transformer oil and reduce the pressure in the tank. We examined the relationship between the position of installation of the pressure-release valve and the pressure on the tank by changing the experimental parameters. We simulated the system with the initial arc occurring at position 2 and measured the pressure at monitoring point 3. We calculated the results when the pressure-release valve was opened at point A directly above the initial arc, at point B directly to its side, and at point C behind the initial arc, as shown in Figure 22. The measured values of the static pressure on the wall under these three conditions are shown in Figure 23.

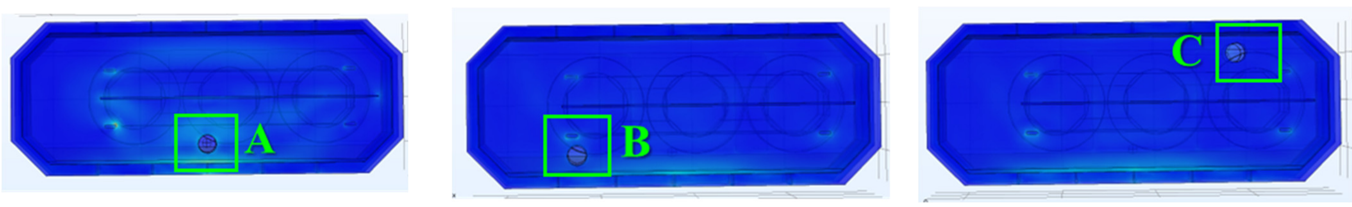

(**a**) Directly above the arc, A (**b**) Front and side, B (**c**) Back, C

Figure 22. Top views of the modeled points A, B, and C at which the pressure-release valve was installed.

Figure 23 shows that installing the pressure-release valve at points A and B reduced the pressure on the wall of the tank, while the pressure on the wall could not be reduced when it was installed at point C. The pressure-release valve had the most prominent effect in terms of reducing the pressure when it was set at point A. The propagation of the transient pressure in this case is shown in Figure 24.

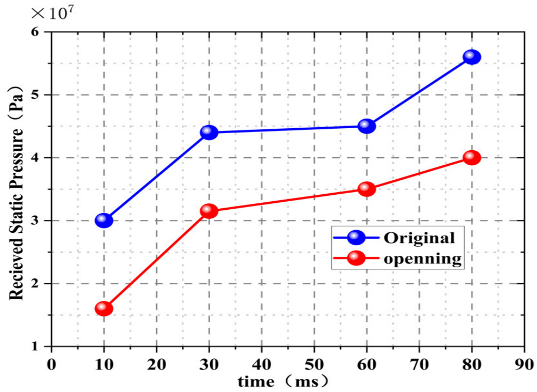

(**a**) A

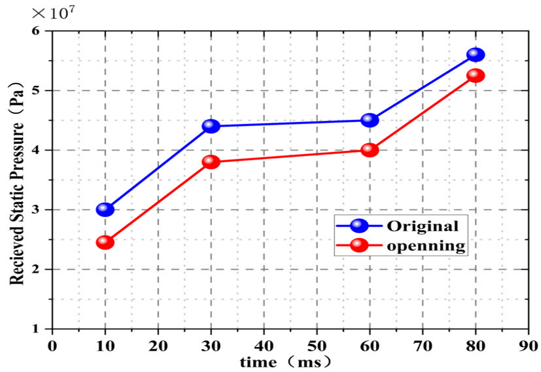

(**b**) B

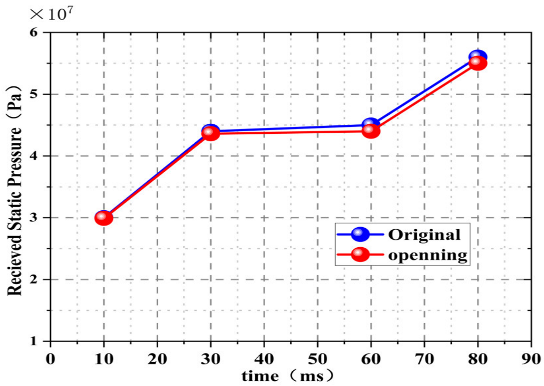

(**c**) C

Figure 23. Diagram of a comparison of pressure when the pressure-release valve was installed at positions A, B, and C.

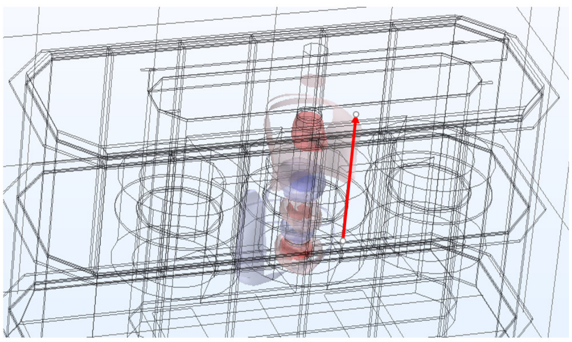

Figure 24. Diagram of propagation of the transient pressure wave (the red arrows represents the direction of pressure propagation).

It is clear from Figure 24 that part of the pressure wave was directly discharged upward through the pressure-release valve rather than spreading around when it was located above the position of occurrence of the arc. This led to a reduction in the pressure on the wall of the tank.

5. Conclusions

We can draw the following conclusions from the above analysis of the inter-turn short-circuit fault inside the transformer tank under the action of an arc discharge, the law of arc development, and the change in the pressure field inside the tank:

(1) The arc energy was related to the initial gas pressure and gas production when the inter-turn short-circuit fault occurred. The pressure wave propagated in the tank and formed backward-traveling waves after interacting with the wall of the tank. The transient pressure at any point in the pipeline was the superposition of the vectors of the forward- and backward-traveling waves.

(2) After the internal failure of the transformer tank, the pressure acting on the wall of the tank continued to increase over time, spreading from the position of the initial arc to all four sides. The tank was deformed, and its side wall closest to the arc expanded 1 ms after the occurrence of the fault. It had distributed through the tank at 20 ms, leading to the expansion and deformation of its entire wall 60 ms after the occurrence of the fault.

(3) The pressure was higher closer to the position of the initial arc. This is because the viscosity of the insulation oil and the internal components of the tank reduced the energy and extent of propagation of the pressure wave.

(4) The pressure-release valve should be installed close to where the arc occurs to reduce the risk of explosion of the tank due to a high pressure.

(5) Combined with the research in this paper, we can develop a pressure warning system to be applied to transformers which can monitor whether there is an explosion risk inside the transformers in real time. This will greatly reduce the occurrence of transformer explosion accidents in production.

Author Contributions: Conceptualization, M.H. and M.Z.; methodology, M.H.; software, Q.Z.; validation, Z.G.; formal analysis, M.H.; investigation, Q.Z.; resources, H.L.; data curation, Z.G. and R.Z.; writing—original draft preparation, M.H.; writing—review and editing, R.Z. and H.L.; visualization, Q.Z.; supervision, M.Z. and H.L.; project administration, Z.G.; funding acquisition, M.Z. All authors have read and agreed to the published version of the manuscript.

Funding: This work is supported by the key project: Research on development law and warning strategy of transformer pressure anomaly, of State grid Shandong Electric Power Company electric power Science Research Institute (2022A-114).

Data Availability Statement: Data are contained within the article.

Conflicts of Interest: Authors Mingming Han, Mengzhao Zhu, Zhaoliang Gu were employed by the company State Grid Shandong Electric Power Company. The remaining authors declare that the research was conducted in the absence of any commercial or financial relationships that could be construed as a potential conflict of interest.

Appendix A

The derivations of select equations are as follows:

Equation (14): Firstly, this equation is derived from the traditional law of heat conduction, and its original equation is:

$$\Delta Q = \mu S(\Delta T/L)$$

μ represents the thermal conductivity coefficient, S represents the heat transfer area of the contact part between the insulating oil and the arc, ΔT represents the magnitude of temperature increase for the insulation oil, and L represents the distance between the insulating oil and the arc during heat conduction.

ΔQ is written as the specific heat capacity representation:

$$\Delta Q = mc_{\text{oil}}\Delta T'$$

where m is the unit mass of the insulating oil, c_{oil} is the specific heat capacity of the insulating oil, and $\Delta T'$ is the temperature difference between the two arc temperatures and the initial insulating oil. Substituting into the above equation, the following can be obtained:

$$\Delta T = \frac{\mu S \Delta T'}{mc_{\text{oil}}L}$$

$$T_{\text{oil}}{}' - T_{\text{oil}} = \frac{\mu S(T_{\text{arc}} - T_{\text{oil}})}{mc_{\text{oil}}L}$$

Expressing ΔT as $T_{\text{arc}} - T_{\text{oil}}$ and $\Delta T'$ as $T_{\text{oil}}{}' - T_{\text{oil}}$ results in Equation (14) in the original manuscript.

Equation (15) is derived based on the traditional energy conversion and phase change reaction laws for the quality of insulating oil that undergoes a phase change reaction. The original equation is:

$$\Delta Q = c_{\text{oil}}m\Delta T + \Delta Q^*$$

Expressing ΔT as $T_{\text{gas}} - T_{\text{oil}}$ and writing ΔQ as the energy transferred by the arc W_{arc} results in Equation (14).

Equation (16) is the Clapeyron equation and does not require derivation.

Equation (17) is obtained by substituting Equation (15) into Equation (16).

Equation (18) is the basic pressure calculation formula, $p = \rho gh$ which describes the relationship between pressure and its density and depth, in addition to its background pressure and initial pressure.

References

1. Chen, G.U.; Peng, L.I.; Huiwen, H.E. Research on DC power transmission technology with voltage level above ±1100 kV. *Proc. CSEE* **2020**, *40*, 6745–6754.
2. Chen, T.; Zhao, L.; Fu, X.; Zhang, J.; Wang, Q.; Hu, C.; Bao, Z.-M.; Li, B.-L.; Li, G. Fire accident characteristics and fire extinguishing scheme of large converter transformers. *Fire Sci. Technol.* **2020**, *39*, 1138–1141.
3. Barnes, M.; Van Hertem, D.; Teeuwsen, S.P.; Callavik, M. HVDC systems in smart grids. *Proc. IEEE* **2017**, *105*, 2082–2098. [CrossRef]
4. Zhao, Z.; Xu, Z.; Wang, J.; Guan, J.; Yu, X.; Li, G. Research on fire safety of large Power transformer. *High Volt. Technol.* **2015**, *41*, 3378–3384.
5. Zhou, Y.-X.; Jiang, X.-X.; Chen, W.-J.; Sha, Y.-C.; Sun, Q.-H.; Zhang, H.-Y. Characteristics of arc discharge and gas production in transformer oil at combined AC-DC voltage. *High Volt. Technol.* **2011**, *37*, 1584–1589.
6. Hwang, J.W.G. Elucidating the Mechanisms Behind Pre-Breakdown Phenomena in Transformer Oil Systems. Master's Thesis, Massachusetts Institute of Technology, Cambridge, MA, USA, 2010.
7. Okabe, S.; Ueta, G.; Wada, H.; Okubo, H. Partial discharge-induced degradation characteristics of oil-impregnated insulating material used in oil-immersed power transformers. *IEEE Trans. Dielectr. Electr. Insul.* **2010**, *17*, 1225–1232. [CrossRef]
8. Li, S.-M.; Li, Q.-Q.; Liu, H.-S.; Yao, J.-Y.; Zhao, Y.-Z.; Han, K.-J. Phase identification of oil paper needle board model under AC-DC combined voltage based on radar spectrum. *Proc. CSEE* **2018**, *38*, 5897–5908+5948.
9. Abi-Samra, N.; Arteaga, J.; Darovny, B.; Foata, M.; Herz, J.; Lee, T.; Nguyen, V.N.; Perigaud, G.; Swinderman, C.; Thompson, R.; et al. Power transformer tank rupture and mitigation: A summary of current state of practice and knowledge by the task force of IEEE power transformer subcommittee. *IEEE Trans. Power Deliv.* **2009**, *24*, 1959–1967. [CrossRef]
10. Wen, J.; Li, Y.; Lin, D.-H.; Tang, F.; Zhang, G.-J. Study on the spatiotemporal Evolution of streamer in Transformer Oil. *Trans. China Electrotech. Soc.* **2019**, *34*, 838–846.
11. Zhu, S.; Wang, S.; Yang, X.; Cheng, X.D.; Zhou, Y. Ignition characteristics of transformer oil under arc action. *Fire Sci.* **2021**, *30*, 142–150.
12. Zhou, J. Dynamic Characteristics and Product Analysis of Natural Ester Insulating Oil Stream Discharge. Master's Thesis, Chongqing University, Chongqing, China, 2019.
13. Mahieu, W.R. Prevention of high-fault rupture of pole-type distribution transformers. *IEEE Trans. Power Appar. Syst.* **1975**, *94*, 1698–1707. [CrossRef]

14. Guo, Z.; Guo, X.; Liu, X.; Jing, C.; Xiao, B.; Lv, D. Research on gas explosion of insulation oil decomposition in substation. *Fire Sci. Technol.* **2018**, *37*, 828–830. (In Chinese)
15. Foata, M.; Iordanescu, M.; Hardy, C. Computational methods for the analysis of explosions in oil-insulated electrical. *IEEE Trans. Power Syst.* **1988**, *3*, 286–293. (In Chinese) [CrossRef]
16. Hamel, A.; Dastous, J.B.; Foata, M. Estimating overpressures in pole-type distribution transformers. I. Tank withstand evaluation. *IEEE Trans. Power Deliv.* **2003**, *18*, 113–119. [CrossRef]
17. Dastous, J.B.; Foata, M.; Hamel, A. Estimating overpressures in pole-type distribution transformers. II. Prediction tools. *IEEE Trans. Power Deliv.* **2003**, *18*, 120–127. [CrossRef]
18. Brodeur, S.; Dastous, J.B. Design and Testing of an Arc Resistant Power Transformer Tank. *IEEE Trans. Power Deliv.* **2020**, *35*, 699–706. [CrossRef]
19. Xiao, L.; Krause, C.; Schlittler, B.; Cukor, I. Verification of Barrier board Over-pressure Withstand Capability and Transformer Operational Risk Mitigation by an Explosion Experiment. In Proceedings of the 2020 8th International Conference on Condition Monitoring and Diagnosis (CMD), Phuket, Thailand, 25–28 October 2020; pp. 310–313.
20. Martin, D.; Beckett, C.; Brown, J.; Nielsen, S. Analysis and mitigation of Australian and New Zealand power transformer failures resulting in fires and explosions. *IEEE Electr. Insul. Mag.* **2019**, *35*, 7–14. [CrossRef]
21. Krasik, Y.E.; Efimov, S.; Sheftman, D.; Fedotov-Gefen, A.; Antonov, O.; Shafer, D.; Yanuka, D.; Nitishinskiy, M.; Kozlov, M.; Gilburd, L.; et al. Underwater Electrical Explosion of Wires and Wire Arrays and Generation of Converging Shock Waves. *IEEE Trans. Plasma Sci.* **2016**, *44*, 412–431. [CrossRef]
22. Muller, S.; Brady, R. Prevention of transformer tank explosion, part 1: Experimental tests on large transformers. In Proceedings of the 2008 ASME Pressure Vessels and Piping Division Conference, Chicago, IL, USA, 27–31 July 2008; pp. 357–365.
23. Han, R.; Zhou, H.; Liu, Q.; Wu, J.; Jing, Y.; Chao, Y.; Zhang, Y.; Qui, A. Generation of Electrohydraulic Shock Waves by Plasma-Ignited Energetic Materials: I. Fundamental Mechanisms and Processes. *IEEE Trans. Plasma Sci.* **2015**, *43*, 3999–4008. [CrossRef]
24. Yao, H.; Lv, K.; Lou, Z.; Xing, M.; Qin, H.; Song, H.; Lv, Z.; Wang, D.; Wang, Z.; Ren, W. Simulation study on oil pressure problems caused by internal faults in oil-immersed transformers. *Process Saf. Environ. Prot.* **2023**, *175*, 190–198. [CrossRef]
25. Bai, S.; Luo, H.; Guan, Y.; Liu, W. Arc Shape and Arc Temperature Measurements in SF_6 High-Voltage Circuit Breakers Using a Transparent Nozzle. *IEEE Trans. Plasma Sci.* **2018**, *46*, 2120–2125. [CrossRef]
26. I Beilis, I.; Koulik, Y.; Boxman, R.L. Temperature Distribution Dependence on Refractory Anode Thickness in a Vacuum Arc: Experiment. *IEEE Trans. Plasma Sci.* **2011**, *39*, 1303–1306. [CrossRef]
27. Marotta, A.; Sharakhovsky, L. Heat transfer and cold cathode erosion in electric arc heaters. *IEEE Trans. Plasma Sci.* **1997**, *25*, 905–912. [CrossRef]
28. Yan, C.; Hao, Z.; Zhang, B. Research on Digital Protection of Transformers Based on Pressure Characteristics. *Chin. J. Electr. Eng.* **2015**, *35*, 6405–6412.
29. Yan, C.G.; Zhang, B.H.; Hao, Z.G.; Chao, G.; Wang, L.; Fu, K.Y.; Liang, D. Modeling and Simulation of Deformation and Rupture of Power Transformer Oil Tank. *J. Electr. Eng. Technol.* **2016**, *31*, 180–187.
30. Jianyi, W.; Yuanxiang, Z.; Huanchao, C. Recent Progress and Prospect of Hydro isomerized Non-naphthenic Transformer Oil. *Proc. CSEE* **2020**, *40*, 5373–5383.
31. Hu, S.; Huang, Z.; Liu, X.; Chen, J.; Wang, Y.; Zhao, T.; Yang, C. Study on High Energy Discharge Characteristics Caused by Arc Faults in Transformer Turret. *IEEE Access* **2023**, *11*, 106924–106933. [CrossRef]
32. Cui, L.; Zhou, Y.; Zhou, X.; Li, Y.; Yang, X. Simulation and Analysis of Pressure Generation Characteristics Caused by Arcing Faults in Transformer. In Proceedings of the 2022 IEEE International Conference on High Voltage Engineering and Applications (ICHVE), Chongqing, China, 25–29 September 2022.
33. Yu, H.; Zhang, Q.; Wang, H.; Ma, S. The performance of the electric locomotive traction transformer insulation oil contrast research. *J. Lubr. Oil* **2016**, *31*, 2328.
34. Zhu, S. Study on Ignition Characteristics of Transformer Insulation Oil under Arc Action. Master's Thesis, University of Science and Technology of China, Hefei, China, 2021.
35. Courant, R.; Friedrichs, K.O.; Lewy, H. On the partial differential equations of mathematical physics. *IBM J. Res. Dev.* **1967**, *11*, 215–234. [CrossRef]